

CHAPTER V

ELECTRORHEOLOGICAL PROPERTIES OF POLYTHIOPHENE/POLYISOPRENE SUSPENSIONS

5.1 Abstract

Electrorheological properties of polythiophene/polyisoprene suspensions were investigated under the oscillatory shear mode and with applied electric field strength varying from 0 to 2 kV/mm. Poly(3-thiophene acetic acid) particles were synthesized via an oxidative polymerization and doped with perchloric acid to control its conductivity. Effects of particle conductivity, and particle concentration under various electric field strengths were investigated. ER responses can be enhanced with increasing electric field strength, particle conductivity, and particle concentration. The storage modulus (G') increased dramatically by 6 orders of magnitude when the electric field strength was increased to 2 kV/mm. These suspensions also exhibited a transition from a fluid-like to a solid-like behavior as the field strength was increased. The influence of particle conductivity and particle concentration were most apparent at intermediate field strength of 0.5 kV/mm. This suggests differences in the polarizability and the particle agglomeration at high field strengths, at high particle conductivity and at high particle concentration. The higher particle conductivity and particle concentration ER fluids possess lower transition field strengths.

Keywords: Electrorheological fluid, Polyisoprene, Polythiophene, Perchloric acid
Dynamic moduli

5.2 Introduction

Electrorheological fluids (ER fluids) are suspensions in which micrometer size polarizable particles are dispersed in an insulating liquid medium. These ER fluids generally exhibit a dramatic change in rheological properties under imposed of AC or DC electric fields [1, 2, 3]. ER fluid, a suspension of silica in kerosene, was

first studied extensively by Winslow (1949), displaying dramatic changes in rheological properties under large applied electric field. The apparent viscosity was strongly increased and a transition to a gel-like phase was obtained at sufficiently high electric fields [4]. When an electric field is imposed, these ER particles become polarized as induced by the mismatches in conductivity and dielectric between the dispersed particles and the continuous medium phase. These fluids show a phase transition from a liquid state to solid state through the interaction between polarized particles and from the formation of a chain-like or fibrilla structure along the direction of the electric field within electrodes. These chains are held together by interparticle forces which have sufficient strength to change the rheological behavior of the material. The particles typically return to an original random orientational distribution and the suspension behaves like liquid-like state after the electric field is removed. These effects are both rapid and reversible [1, 2, 5, 6]. Because of the many desirable characteristics of ER fluids, such as the short response time, the low power consumption, controllable viscosity, the smoothness of operation and mechanical simplicity, ER fluids are useful for the development of many devices, e.g. active engine mounts, shock absorbers, clutches, brakes, damping devices, hydraulic valves, and robotic controlling systems [1, 2, 8].

Various dry-base ER systems with anhydrous particles such as intrinsically polarizable semiconducting polymers and zeolites [1] have been investigated due to their advantages over wet-base ER systems in terms of thermal stability and corrosion of the device [1]. ER materials have recently been developed from using conjugated polymer particles; e.g. conductive polymers as suspended particles for dry-base ER fluid. Conductive polymers can offer a variety of advantages for ER systems: better thermal stability, insolubility, conductivity control. Various conductive polymers have been studied in the ER systems: polyaniline (PANI) and its derivatives [2, 6, 8], and polypyrrole [9]. Polythiophene has several advantages over other semiconducting polymer particles: density, conductivity control, and thermal and environmental stability. It can be easily polymerized by an oxidative polymerization at relatively low temperatures, which gives a high yield and it can be doped from an insulating state to a conducting state by using simple protonic acids.

This allows controlling the particle dielectric constant and conductivity while keeping all other particle properties nearly the same [2, 10, 11, 12].

In this study, we investigated the rheological properties of ER fluids using Poly(3-thiophene acetic acid) (P3TAA) particles doped with perchloric acid (HClO₄) suspended in polyisoprene suspensions. ER properties of P3TAA were investigated under the linear oscillatory deformation mode. We are interested in the effects of particle conductivity and particle concentration on the dynamic moduli under the applied electric field. Moreover, sol-to-gel transition points where the material theoretically changes from the liquid behavior to the solid behavior were determined.

The Electrorheological Effect (ER effect)

Because we are dealing electrorheological fluids, a simplified description of the ER effect is introduced and summarized here. The nature of the ER effect will be explained using the one point dipole approximation. Polarization in the point dipole model occurs not at the surface of the particle but within it. It is generally accepted that the electric field polarizes particles and that the interaction of these induced dipoles provides the forces leading to chain formation or fibrillation and followed by the change in rheological properties [6]. For the ER effect in dc electric fields, the conductivity is important for the ER effect. It is assumed that an ER fluid is composed of spherical particles of conductivity σ_p , suspended in a fluid matrix of conductivity σ_m . When exposed to an external electric field, a mismatch in conductivity between particles and the medium causes polarization of particles, leading to charge separation on particle surfaces [6]. The particle then acquires an induced dipole moment, μ

$$\mu = 4\pi r^3 \epsilon_0 \epsilon_m \beta_\sigma E \quad (5.1)$$

where r is the radius of the particle, ϵ_0 is the permittivity in vacuum ($= 8.854 \times 10^{-12}$ F/m), and E is the intensity of the applied field, and β_σ is the effective conductivity mismatch, as described by [4, 6, 13]:

$$\beta_\sigma = (\sigma_p - \sigma_m) / (\sigma_p + 2\sigma_m) \quad (5.2)$$

As can be seen in equation (5.2), if there is no conductivity mismatch between particles and medium ($\sigma_p = \sigma_m$), there is no effective dipole moment of particles.

When two particles are aligned along the applied electric field and are in contact with each other, the dipole-dipole interaction (F) between two dipole particles is given by the following equation [14]:

$$F = (3/2)\pi r^2 \epsilon_0 \epsilon_m \beta^2 \sigma E^2 \quad (5.3)$$

There are many straight migration paths of dispersed particles in ER fluids, which remain parallel to the direction of the applied field. Assuming that electrostatic interactions between dispersed particles in a path are based only upon an interaction between two adjacent particles and that interaction between other paths of particles are negligible. Macroscopic mechanical properties such as storage and loss moduli can be estimated by multiplying the electrostatic force between adjacent particles at short range in the path. McLeish *et al.* (1991) [15] modeled the microstructure as single-sphere-width chins, most of which were connected to both electrodes. The storage modulus arises from the electrostatic interactions creating tension along the chain. Modeling the electrostatic interactions in the point-dipole limit, the predicted storage modulus as [15];

$$G' = 3\phi\epsilon_0\epsilon_m\beta^2E^2 \quad (5.4)$$

Shiga (1997) [14] reported that an increase in elastic modulus due to an applied electric field ΔG is given as follows [14]:

$$\Delta G = (9/4)\phi\epsilon_m\beta^2E^2 \quad (5.5)$$

where ΔG is change in elastic modulus, ϕ is the volume fraction of particles, ϵ_m is relative dielectric constant of matrix, and E is the intensity of the applied field. This states that ΔG is proportional to ϕ , ϵ_m or E^2 . When these factors reach maximum values, ΔG is expected to become saturated.

5.3 Experimental

5.3.1 Materials

3-thiopheneacetic acid, 3TAA (AR grade, Fluka) was used as the monomer. Anhydrous ferric chloride, FeCl_3 (AR grade, Riedel-delHean) was used as the oxidant. Chloroform, CHCl_3 (AR grade, Lab-Scan), methanol, CH_3OH (AR grade, Lab-Scan) and Dimethyl sulfoxide (DMSO) are dried over CaH_2 for 24 hours under the nitrogen atmosphere and then distilled, were used as solvents. The perchloric acid dopant, HClO_4 (AR grade, AnalaR) was used as received. Sulfuric acid, H_2SO_4 was used to protect the oxidative decomposition of monomer. Diethyl ether and deionized water were used to extract and wash materials. Sodium hydroxide, NaOH was used as the hydrolyzing agent. Polyisoprene, PI ($M_w = 40,000$, viscosity = 400 poise, Aldrich), was used as the host fluid with density 0.92 g/cm^3 .

5.3.2 Instruments

The Fourier transform infrared spectrometer (Thermo Nicolet, Nexus 670) with number of scans of 32, a UV-Visible absorption spectrometer (Perkin Elmer, Lambda 10), a thermalgravimetric analyzer (DuPont, model TGA 2950) with the temperature scan from 30 to 800°C with a heating rate of $10^\circ\text{C}/\text{min}$ under O_2 atmosphere were used to characterize the synthesized polythiophene and polythiophene/polyisoprene blends. A scanning electron microscope (JOEL, model JSM-5200-2AE) was used to determine the morphological structure of the synthesized polymers and polymer blends with the magnifications of 350 and 1,500 and at 20 kV. A custom-built two-point probe electrometer (Keithley, Model 6517A) was used to determine electrical conductivity of conductive polymer. A melt rheometer (Rheometric Scientific, ARES) was used to measure electrorheological properties. A DC power supply (Instek, GFG 8216A), which can deliver electric field strength to $2 \text{ kV}/\text{mm}$.

5.3.3 Synthesis of Poly(3-Thiopheneacetic acid) (P3TAA)

The reaction was by oxidative-coupling polymerization according to the method of Kim *et al.* [16]. 10.0 g of 3-thiopheneacetic acid was refluxed for 24 hours in 50 ml of dry methanol with 1 drop of concentrated H₂SO₄ in order to protect the oxidative decomposition of the carboxylic acid group of monomer during oxidative-coupling polymerization. The methanol was evaporated, and the residue was extracted with fresh diethyl ether. The extract was washed with deionized water, dried with anhydrous MgSO₄ and then filtered. The diethyl ether was evaporated from the filtrate by rotating evaporator.

Thiophene methyl acetate (TMA) product was obtained after the diethyl ether was evaporated from the filtrate by rotating evaporator. In a 100 ml three-necked flask, a solution of 10 mmol of protected monomer in 20 ml of chloroform was added dropwise to a solution of 40 mmol of ferric chloride was dissolved in 30 ml of dry chloroform under nitrogen atmosphere. The molar ratio of the oxidant to monomer is 4:1 in all cases. The reaction was carefully maintained at 0°C ($\pm 0.5^\circ\text{C}$) for 24 hours. The reaction mixture was precipitated, by pouring into a large excess amount of methanol (1 L) to obtain PTMA. The product was repeatedly washed with methanol and deionized water.

PTMA was hydrolyzed as follow; 0.5 g of PTMA was dissolved in 50 ml of 2.0 M NaOH solution and heated for 24 hours at 100°C. The mixture was filtered, neutralized and precipitated with a dilute HCl solution (~0.5 M) to obtain polymer product. The P3TAA was washed several times with deionized water before vacuum drying at room temperature for 2 days.

5.3.4 Doping of Polythiophene

To examine the effect of particle conductivity on the electrorheological properties, P3TAA with different conductivity values were prepared by doping with perchloric acid [17]. The 2.0 M HClO₄ doped P3TAA was prepared by immersing P3TAA particles in 2.0 M HClO₄ solution at room temperature for 3 days. The doping level was varied by varying the mole ratio of the dopant and the monomer, HClO₄/P3TAA (doping ratio equal 1:1, 10:1 and 200:1). The HClO₄ doped P3TAA particles were filtered and vacuum-dried for 24 hours

before grinding with a mortar and pestle and then passed through a 38 μm sieve shaker to control the particle size distribution [3]. After the doping process, their electrical conductivity was studied by using the custom-built two-point probe electrometer (Keithley, Model 6517A).

5.3.5 Preparation of the ER Fluids

The polythiophene powder was sieved with a mesh particle size of 38 μm and dried at room temperature for 24 hours prior to their uses. The electrorheological, ER, fluids were prepared by dispersing undoped and HClO_4 doped P3TAA particles, at various particle concentrations (5, 10, and 20 vol.%) in a polyisoprene fluid (density 0.92 g/cm^3 , and viscosity 400 poise). The prepared ER fluid were then stored in a dessiccator prior to use and then redispersed before each measurement.

5.3.6 Characterization Method

Fourier-transform infrared spectrometer (FT-IR), each poly (3-thiophene acetic acid) sample was identified for functional groups by FT-IR spectrometer Fourier (Thermo Nicolet, Nexus 670) operated in the absorption mode with 32 scans and a resolution of $\pm 4 \text{ cm}^{-1}$, covering a wavenumber range of 4000-400 cm^{-1} using a deuterated triglycine sulfate detector. Optical grade KBr (Carlo Erba Reagent) was used as the background material. The synthesized PTAA was intimately mixed with dried KBr at a ratio of P3TAA: KBr = 1:20. Samples were grounded with a mortar, mixed with KBr and molded into pellets under the pressure of 8 tons.

UV-Vis spectra were recorded with a UV-Vis absorption spectrometer (Perkin-Elmer, Lambda 10). Measurements were taken in the absorbance mode in the wavelength range of 200-800 nm. Synthesized P3TAA was grinded into a fine powder, dissolved in DMSO at the concentration of $6.0 \times 10^{-5} \text{ M}$ and pipetted into the sample holder. Scan speed was 240 mm/min, and a slit width of 2.0 nm using a deuterium lamp as the light source.

The thermal stability of PTAA was investigated using a thermogravimetric analyzer (DuPont, model TGA 2950) in temperature range 30 to 800°C with a heating rate of 10°C/min and O₂ atmosphere [3].

The particle sizes of poly(3-thiophene acetic acid) were determined by using a particle size analyzer (Malvern Instruments Ltd. Masterizer X Version 2.15).

The electrical conductivity of undoped poly(3-thiophene acetic acid) was studied by using the custom-built two-point probe electrometer (Keithley, Model 6517A). The specific conductivity σ (S/cm) values of the pellets were obtained by measuring the bulk pellet resistance R (Ω). The relation $\sigma = (1/Rt)(1/K) = (I/Vt)(1/K)$ was used to calculate specific conductivity, where t is the pellet thickness (cm), I is the current (A), V is the applied voltage (voltage drop) (V), and K is the geometric correction factor which is equal to the ratio w/l , where w and l are the probe width and the length, respectively. The geometrical correction factor (K) was determined by calibrating the two-point probe with semi-conducting silicon sheets of known resistivity values. These two probes were connected to a voltmeter (Keithley, Model 6517A) which supplied a constant voltage source and measured the current. Electrical conductivity values of several samples were first measured at various applied voltages to identify their linear Ohmic regimes. The applied voltage was plotted versus the current change to determine the linear Ohmic regimes of each sample. The applied voltage and the current change in this linear Ohmic regime were converted to the electrical conductivity of polymer using above relation.

5.3.7 Electrorheological Properties Measurement

A Melt rheometer (Rheometric Scientific, ARES) was used to measure rheological properties. It is fitted with a custom-built copper parallel plates fixture (diameter of 25 mm). A DC voltage was applied with a DC power supply (Instek, GFG 8216A), which can deliver electric field strength to 2 kV/mm. A digital multimeter was used to monitor voltage input. In these experiments, the oscillatory shear strain was applied and the dynamic moduli (G' and G'') were measured as functions of frequency and electric field strength. Strain sweep tests were first carried out to determine the suitable strain to measure G' and G'' in the linear viscoelastic regime at a fixed frequency of 1.0 rad/s and at increasing strain

amplitude. The suitable strains in the linear viscoelastic regime are shown in Table 1. Then frequency sweep tests were carried out to measure G' and G'' of each sample as functions of frequency. The deformation frequency was varied from 0.1 to 100 rad/s. To obtain the steady state ER response, the electric field was applied for 10 minutes to ensure the formation of equilibrium polarization and equilibrium agglomerate before each measurement was taken. Each measurement was carried out at the temperature of 27°C and repeated at least two or three times.

5.4 Results and Discussion

5.4.1 Characterization of Poly(3-thiophene acetic acid)

The FT-IR spectrum of the synthesized P3TAA was recorded to identify major absorption peaks as found in previously published work [16]. The characteristic peaks of P3TAA were found at 3200-3000 cm^{-1} , 3000-2800 cm^{-1} , 1700 cm^{-1} , 1300-1200 cm^{-1} and 830 cm^{-1} . These peaks can be assigned to the C-H bond stretching on the thiophene ring; the aliphatic C-H bonds stretching; the carboxylic acid C=O stretching; the thiophene ring stretching; the carboxylic acid C-O stretching, and the out-of-plane thiophene C-H stretching, respectively [16]. The most characteristic feature in this spectrum is the extremely broad O-H absorption occurring in the region from 3400-2400 cm^{-1} , which can be attributed to the strong hydrogen bonding of the dimer. This absorption often obscures the C-H stretching vibrations that occur in the same region. It is obvious from the absorption peak at around 1700 cm^{-1} that the ester groups were not deteriorated during the oxidative polymerization.

The UV-visible absorption spectra of synthesized P3TAA solution in DMSO shows an absorption peaks at 275 nm and 415 nm corresponding to the π - π^* transition of the bithiophene unit, and the polymer backbone, respectively [16, 18]. For HClO_4 doped P3TAA, the spectrum possesses two dominant peaks at 435 nm, and a broad peak at 735 nm, which correspond to the π - π^* transition of the polymer backbone, and the π - π^* transition of the polaron state, respectively [19].

The TGA thermogram of synthesized P3TAA shows two degradation steps at 200°C and 440°C corresponding to the side chain degradation and the backbone degradation, respectively [3]. After doping, the thermograms show the degradation temperature of perchloric acid dopant at around 148°C and a decrease in the thermal stability of main chain as compared to that of the undoped P3TAA.

The mean particle diameter of P3TAA was determined to be approximately 20 μm with standard deviation of 4 μm . The particle microstructure was observed by the scanning electron microscope (SEM). As shown in Fig. 5.1, the shapes of the undoped P3TAA and doped P3TAA particles are quite irregular and the particles have a broad size distribution [3].

The specific conductivity of undoped P3TAA (Pth_U), and HClO_4 doped P3TAA at various doping ratios were measured by the custom-built two probe (Keithley, Model 6517A). The specific conductivity and doping level increase with doping ratios, as shown in Table 5.2, due to the creation of more mobile charges carriers, i.e. an increase in the number of polaron and bipolaron species. As the number of charge carriers increases in P3TAA chains, the electrostatic repulsion leads to changes in chain conformation and thus an increase in the charge carrier mobility [3, 10, 20, 21].

5.4.2 Electrorheological Properties of PT3AA/Polvisoprene Suspensions

The effect of particle conductivity and particle concentration on the electrorheological properties of P3TAA/Polyisoprene suspensions (Pth/PI) were investigated. The properties of P3TAA particles are shown in Table 5.2. To study the effect of particle conductivity, the particle concentration was fixed at 5 vol.% and the particle conductivity value were set at 3.01×10^{-6} , 1.54×10^{-3} , 3.66×10^{-3} , and 1.12×10^{-1} S/cm for Pth_U, Pth_1:1, Pth_10:1, and Pth_200:1 suspensions, respectively. Particle concentrations investigated were 5, 10, and 20 vol.% at a specific conductivity of 1.12×10^{-1} S/cm (5Pth_200:1/PI, 10Pth_200:1/PI, and 20Pth_200:1/PI). The dynamic moduli, G' and G'' , were measured in the linear viscoelastic regime at appropriate strains as a function of deformation frequency as shown in Table 5.1.

5.4.2.1 Effect of Particle Conductivity

The effect of particle conductivity on the electrorheological properties of P3TAA/polyisoprene suspensions (Pth/PI) was first investigated as a function of frequency in the range of electric field strength between 0-2 kV/mm, and the particle concentration was fixed of 5 vol.%. The particle conductivity were 3.01×10^{-6} , 1.54×10^{-3} , 3.66×10^{-3} , and 1.12×10^{-1} S/cm for Pth_U/PI, Pth_1:1/PI, Pth_10:1/PI, and Pth_200:1/PI, respectively. Figures 5.2(a) and 5.2(b) show the effect of particle conductivity to storage and loss moduli (G' and G'') of the suspensions. The influence of particle conductivity is evident at the moderate field strength (0.5 kV/mm); G' and G'' of the 5Pth_200:1/PI suspensions are substantially larger than the lower conductivity systems. $G'(\omega)$ of the 5Pth_200:1/PI suspensions increase dramatically by 5 order of magnitude and $G''(\omega)$ also increase but much less than $G'(\omega)$ as the electric field was applied up to 2 kV/mm. Figures 5.3(a) and 5.3(b) show the storage and loss modulus responses ($\Delta G'$, and $\Delta G''$) of various particle conductivities as a function of electric field strengths obtained at frequency of 1.0 rad/s. The storage and loss modulus responses appear to generally increase at high field strength (0.5-2 kV/mm). The responses are proportional to the square of the applied electric field at electric field strengths of 1.5 and 2 kV/mm corresponding to the typical correlation of the change in elastic modulus (ΔG) and the electric field strength (E) as follows [14]; $\Delta G = (9/4)\phi\epsilon_m\beta^2\sigma E^2$. At lower electric field strengths (0.5-1 kV/mm), the responses increase with electric field strengths with an even higher exponent. The 5Pth_200:1/PI system possesses the highest storage and loss modulus responses. The storage modulus response values at electric field strength of 2 kV/mm were 4326, 4648, 7980, and 11272 Pa for 5Pth_U/PI, 5Pth_1:1/PI, 5Pth_10:1/PI, and 5Pth_200:1/PI, respectively. The loss modulus response values at electric field strength of 2 kV/mm were 2591, 1712, 2305, and 3791 Pa for 5Pth_U/PI, 5Pth_1:1/PI, 5Pth_10:1/PI, and 5Pth_200:1/PI, respectively. Figures 5.4(a) and 5.4(b) show the storage and loss modulus responses as a function of doping ratio at electric field strengths of 1 and 2 kV/mm. The dynamic moduli responses appear to increase nonlinearly with doping level.

These results suggest the mechanism for the ER effect in particulate dispersions that, in the absence of the electric field, the particles are randomly dispersed in the suspensions under the influence of the Brownian force. The system showed a liquid-like behavior in which G'' is larger than G' [3, 22]. Under the action of an electric field, the particles become polarized creating induced dipole moment, leading to interparticle attractions which result in the formation of chain-like or fibril agglomerates in the direction of electric field [3, 7]. The microstructures change from the disordered state to an ordered state and the suspensions become to show solid-like behavior. Higher electric field strength induces a higher dipole moment and causes particle chains to pull themselves together tighter due to the greater electrostatic force and form thicker chains [23]. These thicker and stronger particle agglomerates result in high rigidity as can be represented by the dramatically increasing in both G' and G'' with electric field strength [3]. The ER fluid would not show any ER effect until the applied electric field strength is larger than the critical one [3, 7] corresponding to the electric field strength of 0.5 kV/mm in our experiment. The increase in the ER response with particle conductivity can be attributed to the creation of more mobile charges carriers and polarizability of particulate in suspension. Increasing in particle polarizability, the resulting attractive forces increase the electrostatic interaction [2, 3, 7].

Particle conductivity effect has been recently reported by others researchers. Chotpattananont *et al.* (2003) [3] reported that the dynamic moduli of polythiophene/polydimethylsiloxane suspensions increased with doping level and increased dramatically by 10 order of magnitude, when the field strength is increased to 2 kV/mm. Block *et al.* [24] studied the particle conductivity influences the ER effect by using the acene-quinone polymer/silicone oil and found that the static yield stress peaked at a particle conductivity of approximately 10^{-5} S/cm.

5.4.2.2 Effect of Particle Concentration

The effect of HClO_4 doped polythiophene particle concentration on the electrorheological properties of P3TAA/PI suspensions was next investigated. In Pth_200:1 system, with the highest specific conductivity of 1.12×10^{-1} S/cm was chosen due to it exhibits the maximum G' responses amongst the various particle conductivity studied. Polythiophene particle concentrations

studied were 5, 10, and 20 vol.% (5Pth_200:1/PI, 10Pth_200:1/PI, and 20Pth_200:1/PI). Figures 5.5(a) and 5.5(b) show the comparisons of the storage modulus (G') and the loss modulus (G'') vs. frequency between Pth_200:1/PI suspensions at different particle concentrations, at electric field strengths of 0, 0.5 and 2 kV/mm. In the absence of electric field, at each concentration, the dynamic moduli, G' and G'' , are of comparable magnitude. The effect of particle concentration becomes apparent at the moderate field strength (0.5 kV/mm), in that G' and G'' of the 20Pth_200:1/PI suspensions are significantly higher than those of 5Pth_200:1/PI. $G'(\omega)$ of the 20Pth_200:1/PI suspensions increase by 6 order of magnitude and $G''(\omega)$ also increase but much less than $G'(\omega)$ as the electric field was applied up to 2 kV/mm. In comparison with the lower concentration suspensions (5Pth_200:1/PI), the dynamic moduli of 20Pth_200:1/PI are higher by about 1 order of magnitude. Figures 5.6(a) and 5.6(b) show the storage and loss modulus responses of various particle concentrations as a function of electric field strength obtained at frequency of 1.0 rad/s. The storage and loss modulus responses appear to generally increase at high field strength (0.5-2 kV/mm) and the dynamic moduli responses of 10Pth_200:1/PI and 20Pth_200:1/PI are proportional to the square of the applied electric field corresponding to the typical relation as follow [14]; $\Delta G = (9/4)\phi\epsilon_m\beta_\sigma^2 E^2$. The 20Pth_200:1/PI exhibited the highest storage and loss modulus responses. The storage modulus response values at electric field strength of 2 kV/mm and frequency of 1.0 rad/s were 11272, 18562, and 75699 Pa for 5Pth_200:1/PI, 10Pth_200:1/PI, and 20Pth_200:1/PI, respectively. The loss modulus response values at electric field strength of 2 kV/mm were 3791, 7174, and 27828 Pa for 5Pth_200:1/PI, 10Pth_200:1/PI, and 20Pth_200:1/PI, respectively. Figures 5.7(a) and 5.7(b) show the storage and loss modulus responses vs. particle volume fractions at electric field strengths of 1 and 2 kV/mm. The dynamic moduli responses appear to increase linearly with volume fraction at low volume fractions (0.05-0.1) but nonlinearly at higher volume fractions (0.2).

These results suggest that the fibrous aggregate sizes depend on the concentration. At low particle concentrations, the microstructures consist mainly of single sphere width chains. As concentration is increased, the number density of chains increases resulting in a denser particle structure organized in the

electric field and the structure consists mainly of thick clusters; there are more agglomerates and fibrillation. These larger agglomerates result in higher rigidity and higher flow resistance as indicated by a higher G' [5, 25].

Chotpattananont *et al.* (2003) [3] reported that the dynamic moduli of polythiophene/polydimethylsiloxane suspensions increased with particle concentration. The higher concentration suspensions show the higher dynamic moduli values and the ER properties reached saturations at a field strength of 1 kV/mm, since G' and G'' were independent of particle concentration. Hao *et al.* [26] have reported that the electrorheological properties (the complex viscosity η^* , the real modulus G' and the imaginary modulus G'') increased sharply once the particle volume fraction exceeds a critical value (ϕ_c) and did not change with the applied electric field strength.

5.4.3 Sol-gel Transition

The sol-gel transition was investigated as the critical field strength where G' becomes larger than G'' at low deformation frequency (0.1-1.0 rad/s). At the sol to gel point, theory and experiment indicate that the frequency dependence of G' and G'' each exhibit identical power law behavior, i.e. that $G' = A\omega^{n'}$ and $G'' = B\omega^{n''}$, with $n' = n''$, and where A and B are related to the gel strength factors [27, 28]. The sol-gel transition point of an ER fluid can be determined by plotting the viscoelastic exponents, n' and n'' as a function of field strength, and observing a crossover where $n' = n'' = n_c$ at critical electric field strength (E_c) [27, 28].

In Figure 5.8(a), both n' and n'' values at low deformation frequency (0.1-1.0 rad/s) were plotted as a function of the applied field strength for the 5Pth_U/PI, and 5Pth_200:1/PI suspensions. Each suspension exhibits a sol-to-gel transition as the electric field increases. For 5Pth_U/PI suspensions, the transition occurs at higher field strength ($E_c = 0.6$ kV/mm, and $n_c = 0.72$) than that of 5Pth_200:1/PI ($E_c = 0.4$ kV/mm, and $n_c = 0.84$). This result points out that the higher particle conductivity is correlated with the lower critical field strength (E_c) for the sol-to-gel transition to occur.

In Figure 5.8(b), both n' and n'' values at low deformation frequency (0.1-1.0 rad/s) were plotted as a function of the applied field strength for the 5Pth_200:1/PI, and 20Pth_200:1/PI suspensions. Again, each suspension shows a transition from a fluid-like to a solid-like behavior. The 20Pth_200:1/PI suspension shows a transition at lower field strength ($E_c = 0.25$ kV/mm, and $n_c = 0.88$). This result suggests that the higher particle concentration is correlated with the lower critical field strength for the sol-to-gel transition to occur.

Winter et al. (2002) [22] reported the sol-to-gel transition of silica/PDMS suspensions through a state with frequency independent $\tan\delta$ as expected for the classical gelation. They found that the critical field strength (E_c) was even lower with increasing volume fraction of particle; $E_c = 60$ V/mm for volume fraction of 0.051 and $E_c = 30$ V/mm for volume fraction of 0.107. Whereas the highest concentration (0.171) did not exhibit such gelation, the slope of $\tan\delta$ was already positive without electric field, due to the possible formation of water-bridges between the more closely packed particles.

5.4.4 Time Dependence of the Electrorheological Response

Finally, we investigated the temporal characteristic of HClO₄ highly doped polythiophene/polyisoprene suspensions (Pth_200:1/PI), during a time sweep test, in which an electric field was turned on and off alternately. The temporal characteristic of each sample was recorded in the linear viscoelastic regime at a strain of 80% and frequency of 1.0 rad/s. Figure 5.9(a) shows the temporal responses of 20Pth_200:1/PI suspensions at electric field strength of 0.5, 1.0 and 2.0 kV/mm. When the electric field was applied, G' immediately increased and subsequently reached a steady state value. After G' reached an equilibrium value, the electric field was turned off. G' of suspensions decreased instantaneously, but it did not recover to its original value. These behaviors indicate that there were some irreversible agglomerations possibly due to some hydrogen bonding between adjacent particles [3]. As with the field-on modulus, the field-off modulus increases with the applied field strength, this suggests that the higher field strength induces higher interparticle forces and larger fibrillation or network structure along the field direction; the

residual interparticle forces are higher when higher fields have been applied [3, 7]. The time required for G' to reach the steady-state value on applying the field is called the induction time, t_{ind} , which was found to be essentially independent of the field strength; 62, 65 and 67 sec at electric field strength of 0.5, 1.0 and 2.0 kV/mm, respectively. The time required for G' to reach a steady-state value when the electric field is turned off is called the recovery time, t_{rec} , which was found to be increase with increasing field strength; 70, 170, and 206 sec at electric field strength of 0.5, 1.0 and 2.0 kV/mm, respectively, as shown in Table 5.3. The independence of t_{ind} with the field strength suggests that the field strength may reflect that the solvent is passive to the electric field thus the particle diffusivity did not change when the field strength is varied [3]. The t_{rec} increases with increasing field strength suggest that the longer times are required to disperse a thicker chain-like structure.

Figure 5.9(b) shows the comparison of the temporal responses of 5Pth_U/PI, 5Pth_200:1, and 20Pth_200:1/PI suspensions at electric field strength of 2 kV/mm. It is evident that the field on and off modulus vary with particle concentration and specific conductivity; a system with a higher concentration and a higher specific conductivity possesses a higher agglomeration. The field on and off modulus of the 20Pth_200:1/PI system shows the highest values. We found that t_{ind} is independent of specific conductivity; 34 and 33 sec for 5Pth_U/PI and 5Pth_200:1/PI, respectively, whereas t_{ind} increases with increasing particle concentration; 33 and 67 sec for 5Pth_200:1/PI and 20Pth_200:1/PI, respectively. t_{rec} is longer at a higher particle concentration and a higher conductivity; 62, 173, and 206 sec for 5Pth_U/PI, 5Pth200:1/PI, and 20Pth_200:1/PI, respectively. These results suggest that the higher particle concentration and conductivity results in thicker agglomerates and fibrillation thus a longer time is required to disperse bigger fibrillation.

5.5 Conclusions

In this study, electrorheological properties (ER properties) of polythiophene/polyisoprene suspensions were investigated by examining the effects of particle conductivity and particle concentration at electric field strength varying from 0 to 2 kV/mm under the oscillatory shear mode. Poly(3-thiophene acetic acid) particles were synthesized via an oxidative polymerization and doped with perchloric acid. The results show that the ER responses can be enhanced with increasing electric field strength, particle conductivity, and particle concentration. The storage modulus (G') increased dramatically by 6 orders of magnitude when the electric field strength was increased to 2 kV/mm. This suspension exhibited a transition from a fluid-like to a solid-like behavior as the field strength was increased. The influence of particle conductivity and particle concentration are most apparent at intermediate field strength of 0.5 kV/mm. This suggests differences in the polarizability and the particle agglomeration at high conductivity, and high particle concentration. In the absence of the electric field, the particles were randomly dispersed in the suspensions. The particles became polarized creating induced dipole moment, leading to interparticle attractions which resulted in the formation of chain-like or fibril agglomerates in the direction of electric field. Higher electric field strength, particle conductivity and particle concentration induced a higher dipole moment and caused particle chains to pull themselves together tighter and formed thicker agglomerates or more fibrillation. The higher particle conductivity and particle concentration resulted in the lower sol-to-gel transition field strength.

5.6 Acknowledgements

The authors would like to acknowledge the financial supports to A.S from Chulalongkorn University (through a grant from the Ratchadapesak Somphot Endowment Fund for the foundation of the Conductive and Electroactive Polymers Research Unit), and the Petroleum and Petrochemical College Consortium.

5.7 References

- [1] Choi, H.J., Cho, M.S., Chin, I.-J., and Ahn, W.-S., *Microporous and Mesoporous Materials* 32 (1999) 233.
- [2] Lee, Y.H., Kim, C.A., Jang, W.H., Choi, H.J., and Jhon, M.S., *Polymer* 42 (2001) 8277.
- [3] Chotpattananont, D., Sirivat, A., and Jamieson, A.M., *Colloid Polym Sci* 282 (2004) 357.
- [4] Atten, P., Boissy, C., and Foulc, J.-N., *Journal of Electrostatics* 40 & 41 (1997) 3.
- [5] Parthasarathy, M., and Klingenberg, D.J., *Materials Science and Engineering* R17 (1996) 57.
- [6] Krause, S., and Bohon, K., *Macromolecules* 34 (2001) 7179.
- [7] Hao, T., *Advances in Colloid and Interface Science* 97 (2002) 1.
- [8] Choi, H.J., Kim, T.W., Cho, M.S., Kim, S.G., and Jhon, M.S., *European Polymer Journal* 33 (1997) 699.
- [9] Goodwin, J.W., Markham, G.M., and Vincent, B., *J. Phys. Chem.* 101 (1997) 1961.
- [10] Kumar, D., and Sharma, R.C., *European Polymer Journal* 34 (1998) 1053.
- [11] Mu, S., and Park, S.M., *Synthetic Metals* 69 (1995) 311.
- [12] Anquetil, P.A., Yu, H., Madden, J.D., Madden, P.G., Swager, T.M., and Hunter, I.W., *Proceedings of SPIE* 4695 (2002) 424.
- [13] Liu, B., and Shaw, T.M., *Journal of Rheology*. 45(3) (2001) 641.
- [14] Shiga, T. *Advances in Polymer Science*, vol.134, Springer-Verlag Berlin Heidelberg, 1997.
- [15] McLeish, T.C.B., Jordan, Y., Shaw, M.T., *J. Rheol.* 35(3) (1991) 427.
- [16] Kim, B., Chen, L., Gong, J.P., and Osada, Y., *Macromolecules* 32 (1999) 3964.
- [17] Kim, B., Chen, L., Gong, J.P., Nishino, M., and Osada, Y., *Macromolecules* 33 (2000) 1232.
- [18] Wang, F., Lai, Y.-H., and Han, M.-Y., *Macromolecules* 37 (2004) 3222.
- [19] Demanze, F., Yassar, A., and Garnier, F., *Macromolecules* 29 (1996) 4267.

- [20] Chandrasekhar, P., *Fundamentals and Applications of Conducting Polymers Handbook*, USA: Kluwer Academic Publishers, 1999.
- [21] Van Vught, F.A. *Transparent and conductive polymer layers by gas plasma techniques*. The Netherlands: L.M.H. Groenewoud, 2000.
- [22] Winter, H.H., and Chin, B.D., *Rheol Acta*, 41 (2002) 265.
- [23] Davis, L.C. *J. App. Phys.* 72(4) (1992) 1334 .
- [24] Block, H., Kelley, J.P., Qin, A., and Watson, T., *Langmuir* 6 (1990) 6.
- [25] Lengalova, A.; Pavlinek, V.; Saha, P.; Quadrat, O.; Kitano, T.; Stejskal, J. *Euro. Polym. J.* 39 (2003) 641.
- [26] Hao, T., Chen, Y., Xu, Z., Xu, Y., Huang, Y., and Chin., *J. Polym. Sci.* 12 (1994) 97.
- [27] Hsu, S.-H; Jamieson, A.M., *Polymer* 34(12) (1993) 2602.
- [28] Nystrom, B.; Walderhaug, H; Hansen, F.K., *Langmuir* 11 (1995) 750.

Table 5.1 Appropriate stain (%) in the linear viscoelastic regime of each system

Systems	Particle concentration (vol.%)	Appropriate strain (%)			
		E (kV/mm)			
		0 - 0.2	0.5	1	1.5 - 2
5Pth U/PI	5	220	10	2	0.7
5Pth 1:1/PI	5	220	2	2	0.3
5Pth 10:1/PI	5	220	2	0.5	0.3
5Pth 200:1/PI	5	220	2	0.5	0.3
10Pth 200:1/PI	10	80	2	0.5	0.3
20Pth 200:1/PI	20	50	0.7	0.5	0.3

Table 5.2 Properties of P3TAA particles

Code	Doping level [ClO ₄]/[S]	Specific conductivity (S/cm)	β_{σ} $[(\sigma_p - \sigma_m)/(\sigma_p + 2\sigma_m)]$	Particle diameter (μm)
Pth U	0.00	$3.01 \times 10^{-6} \pm 1.01 \times 10^{-7}$	0.472	19.13 ± 3.14
Pth 1:1	0.0427 ± 0.0060	$1.54 \times 10^{-3} \pm 3.72 \times 10^{-4}$	0.998	17.66 ± 0.51
Pth 10:1	0.1593 ± 0.0736	$3.66 \times 10^{-3} \pm 2.00 \times 10^{-4}$	0.999	17.00 ± 0.53
Pth 200:1	0.2089 ± 0.0402	$1.12 \times 10^{-1} \pm 1.53 \times 10^{-2}$	0.999	23.56 ± 0.21

Note β_{σ} is conductivity mismatch, σ_p is the conductivity of particle, σ_m is the conductivity of matrix (polyisoprene fluid = $8.18 \times 10^{-7} \pm 1.13 \times 10^{-7}$ S/cm)

Table 5.3 Induction time and recovery times at 27°C of doped and undoped polythiophene/polyisoprene suspensions

Samples	Electric field (kV/mm)	Induction time (τ_{ind}) (s)	Recovery time (τ_{rec}) (s)	$\Delta G'_{ind}$ (Pa)	$\Delta G'_{rec}$ (Pa)	$\Delta G''_{ind}$ (Pa)	$\Delta G''_{rec}$ (Pa)
5Pth U/PI	2.0	34	62	25	24	148	122
5Pth 200:1/PI	2.0	33	173	61	57	303	277
20Pth_200:1/PI	0.5	62	70	10	8	89	61
	1.0	65	170	35	32	271	232
	2.0	67	206	133	125	772	699

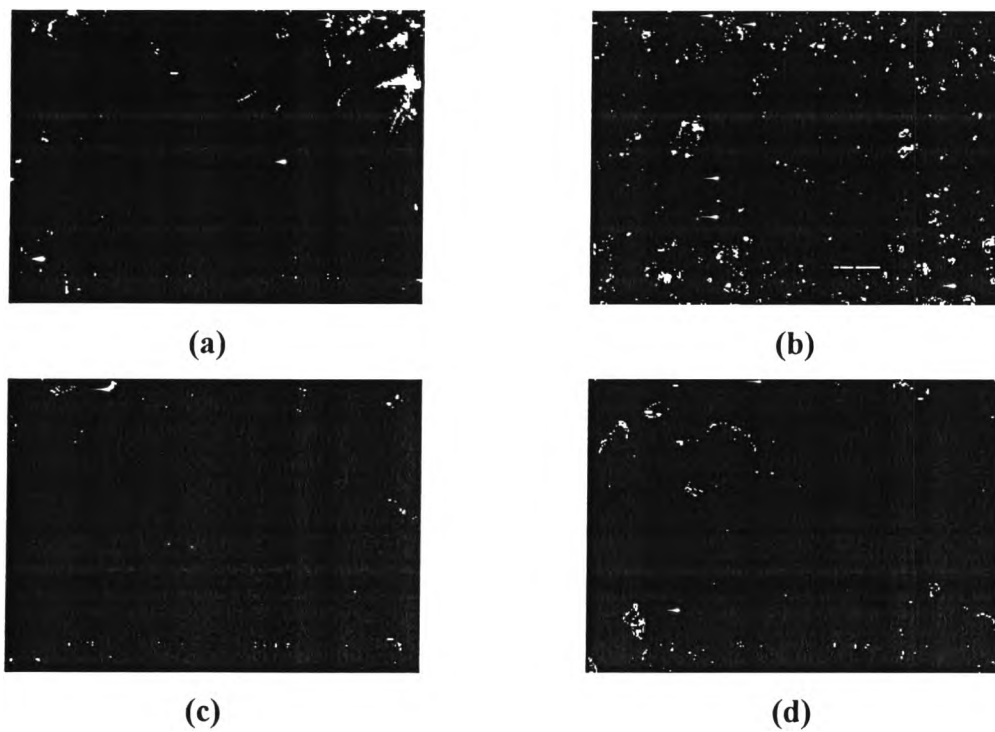
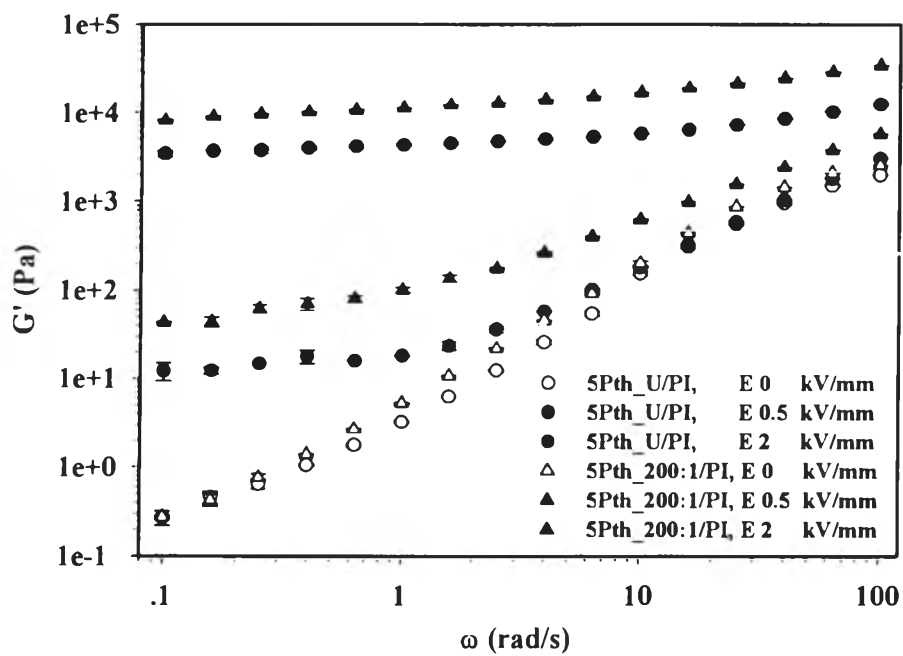
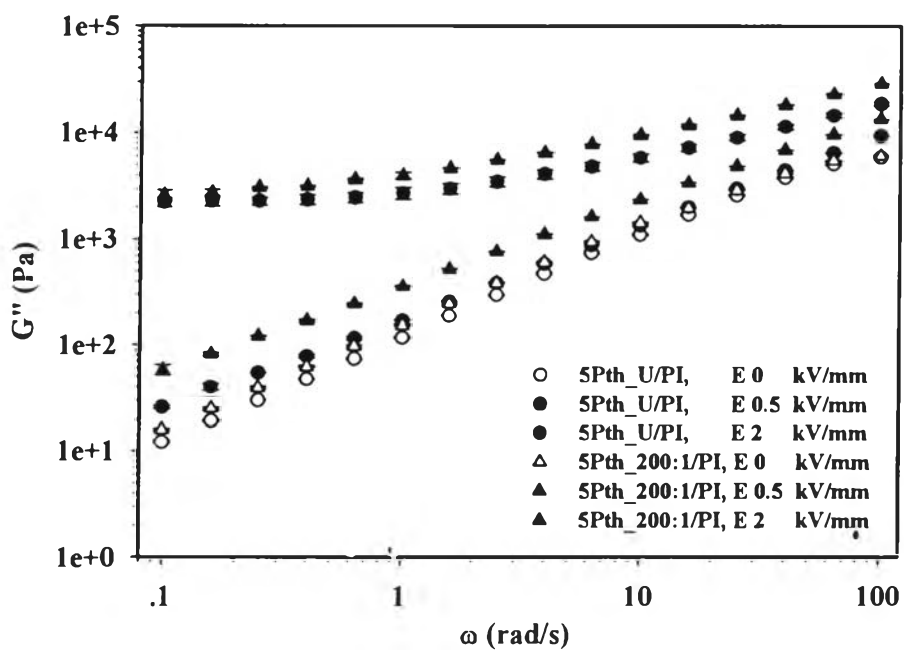


Figure 5.1 The morphology of HClO_4 doped polythiophene at various doping ratios: a) Pth_U; b) Pth_Pth_1:1; c) Pth_10:1; d) Pth_200:1 at magnification of 1,500.

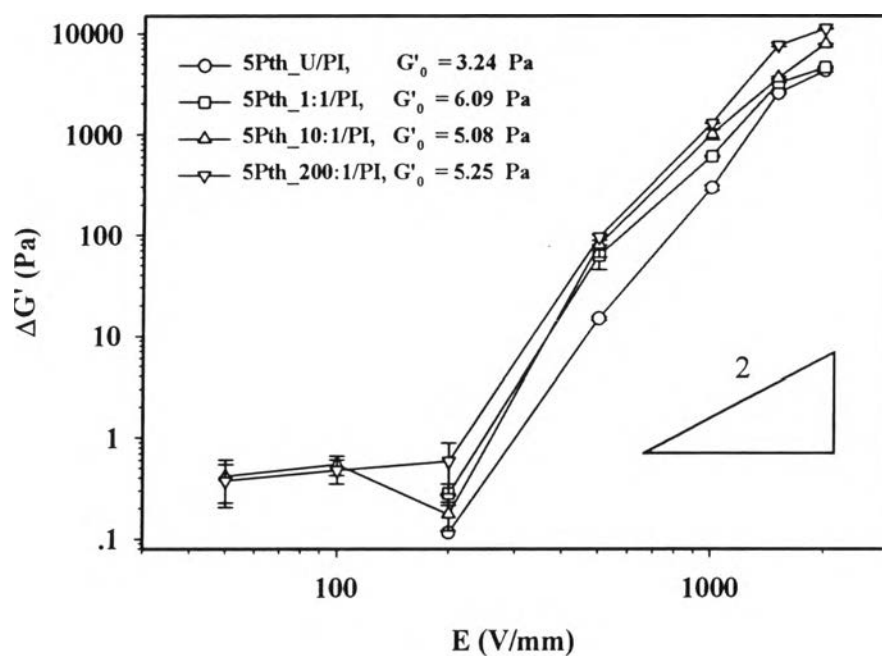


(a)

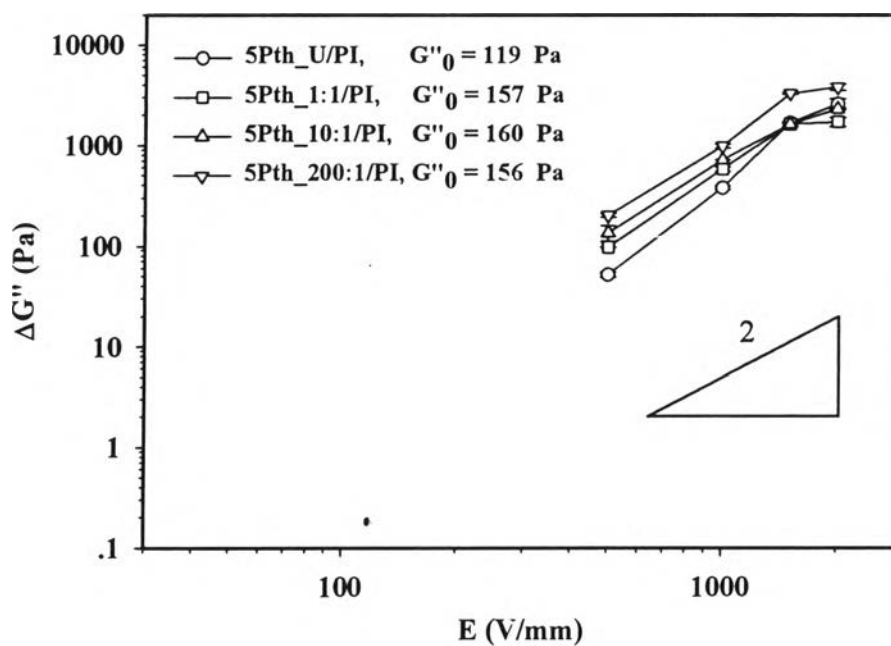


(b)

Figure 5.2 Storage and loss moduli of 5vol.% polythiophene/polyisoprene suspensions (5Pth/PI) at various doping ratios vs. frequency, 27°C: (a) storage modulus, $G'(\omega)$; (b) loss modulus, $G''(\omega)$.

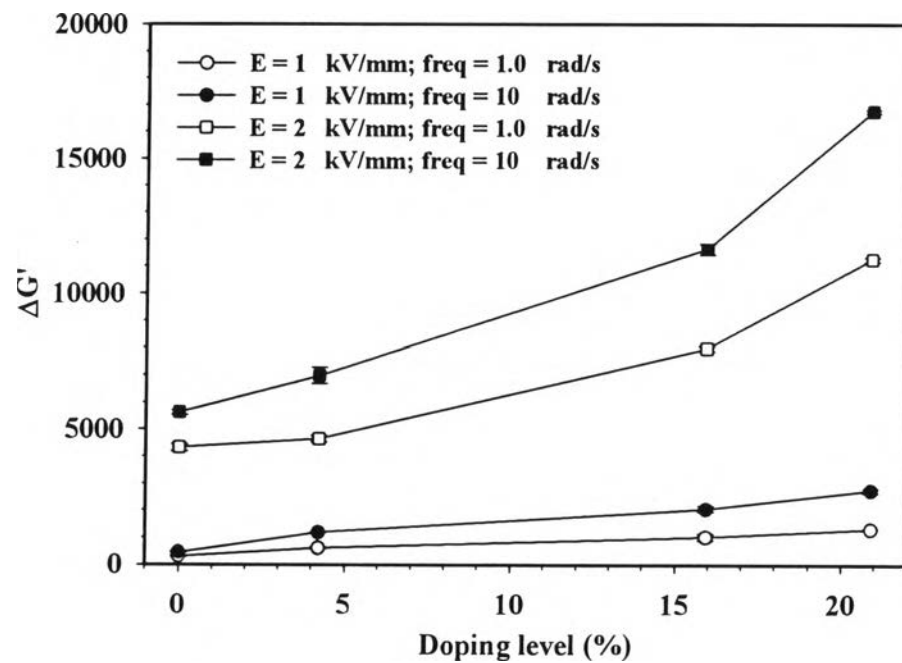


(a)

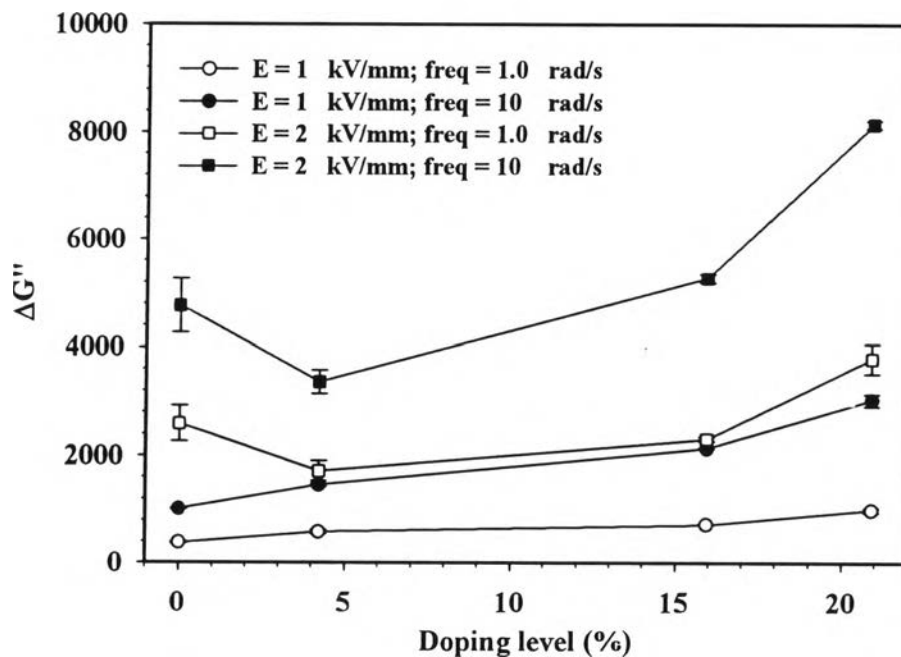


(b)

Figure 5.3 Storage modulus ($\Delta G'$) and loss modulus responses ($\Delta G''$) of 5vol.% polythiophene/polyisoprene suspension (5Pth/PI) at various doping ratios vs. electric field strength, at frequency of 1.0 rad/s, and at 27⁰C: (a) storage modulus response; (b) loss modulus response, which the data below 0.4 kV/mm are negligible.

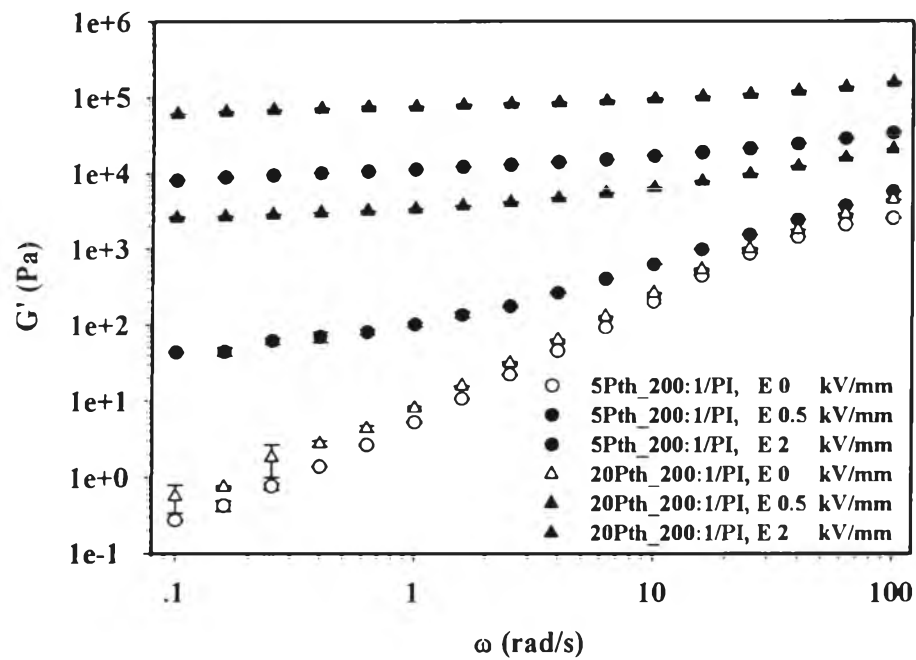


(a)

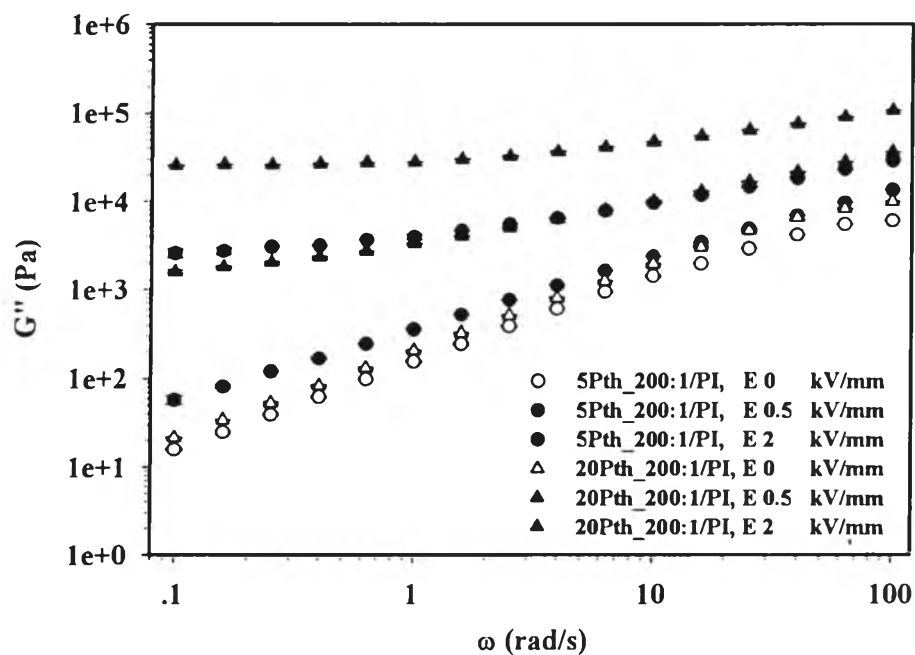


(b)

Figure 5.4 Storage modulus ($\Delta G'$) and loss modulus responses ($\Delta G''$) of doped polythiophene/polyisoprene suspensions as functions of doping level, 27°C, at various frequencies, and at electric field strengths of 1 and 2 kV/mm.

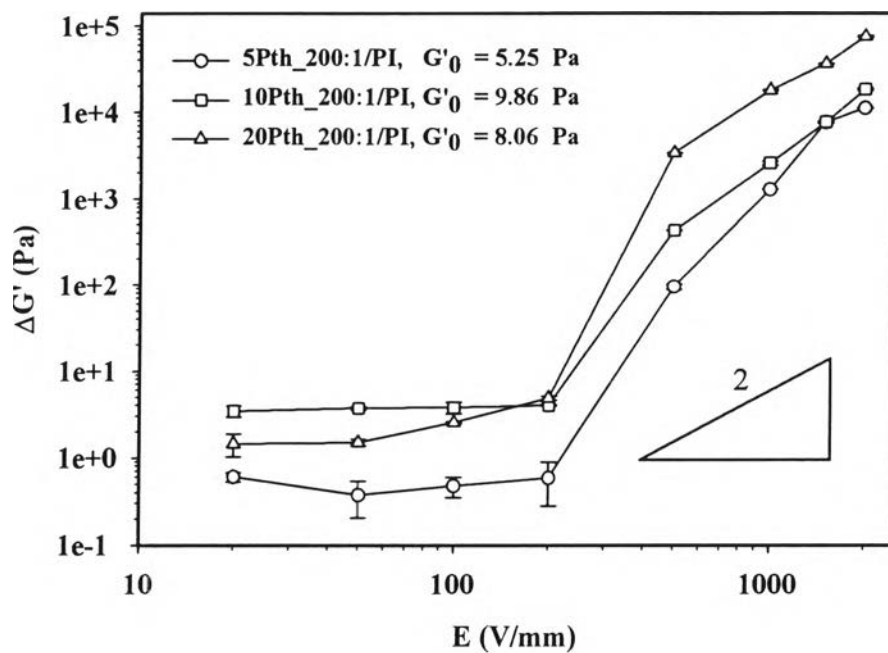


(a)

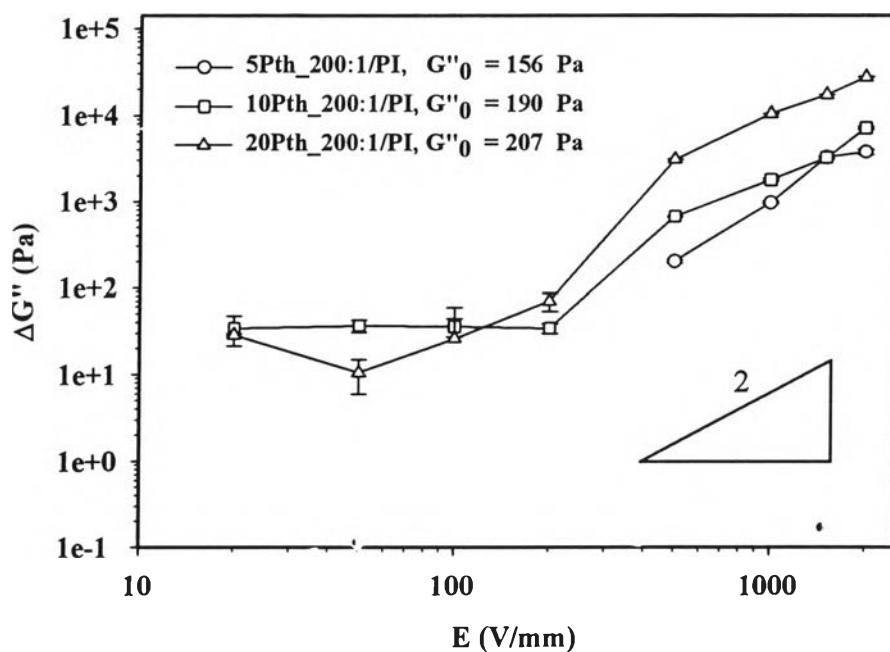


(b)

Figure 5.5 Storage and loss modulus of HClO_4 highly doped polythiophene/polyisoprene suspensions (Pth_200:1/PI) at various particle concentrations vs. frequency, 27°C : (a) storage modulus, $G'(\omega)$; (b) loss modulus, $G''(\omega)$.

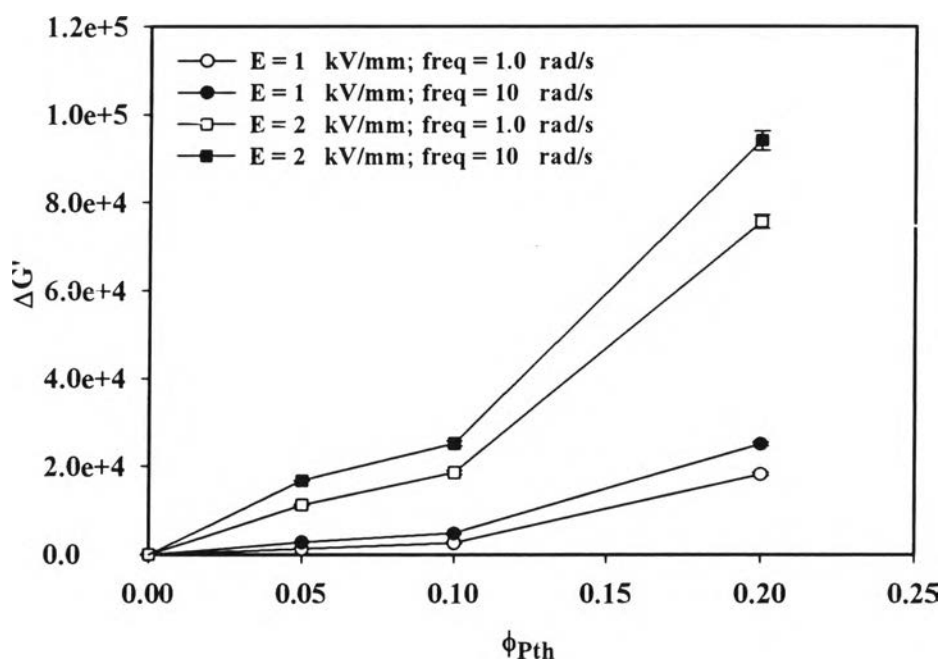


(a)

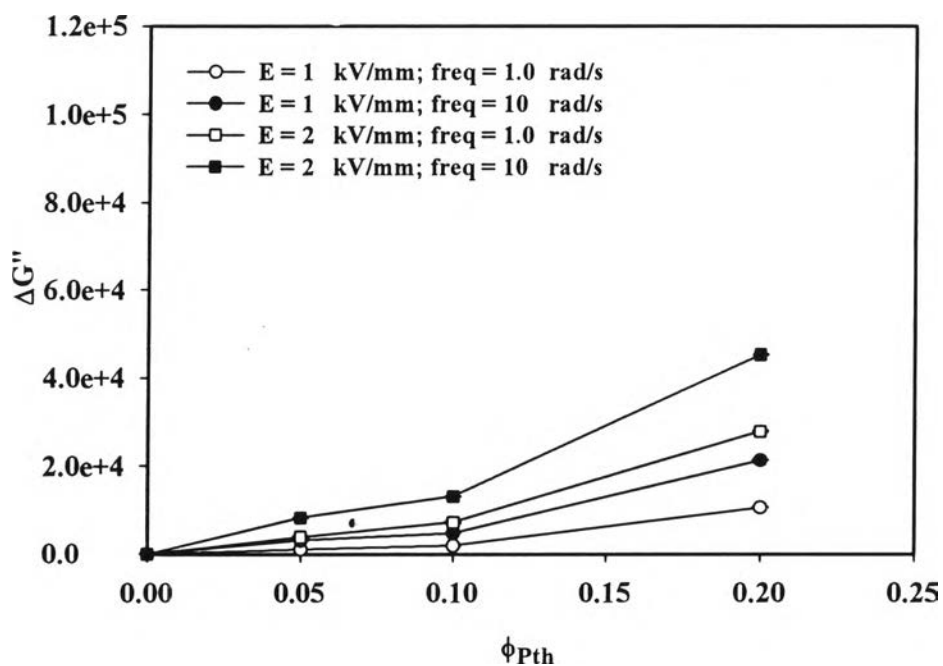


(b)

Figure 5.6 Storage modulus ($\Delta G'$) and loss modulus responses ($\Delta G''$) of HClO_4 highly doped polythiophene/polyisoprene suspensions (Pth_200:1/PI) at various particle concentrations vs. electric field strength, at frequency of 1.0 rad/s, at 27°C : (a) storage modulus responses; (b) loss modulus responses.

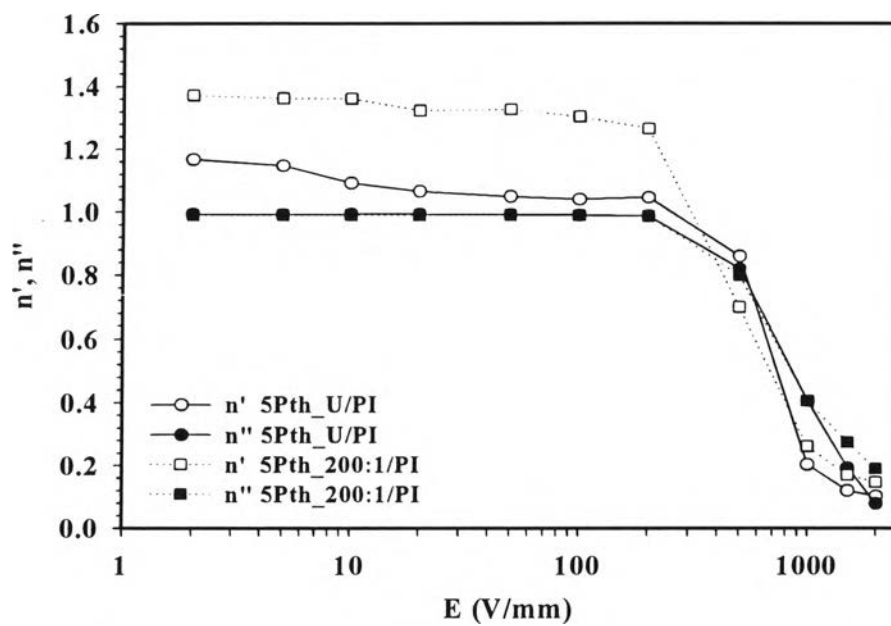


(a)

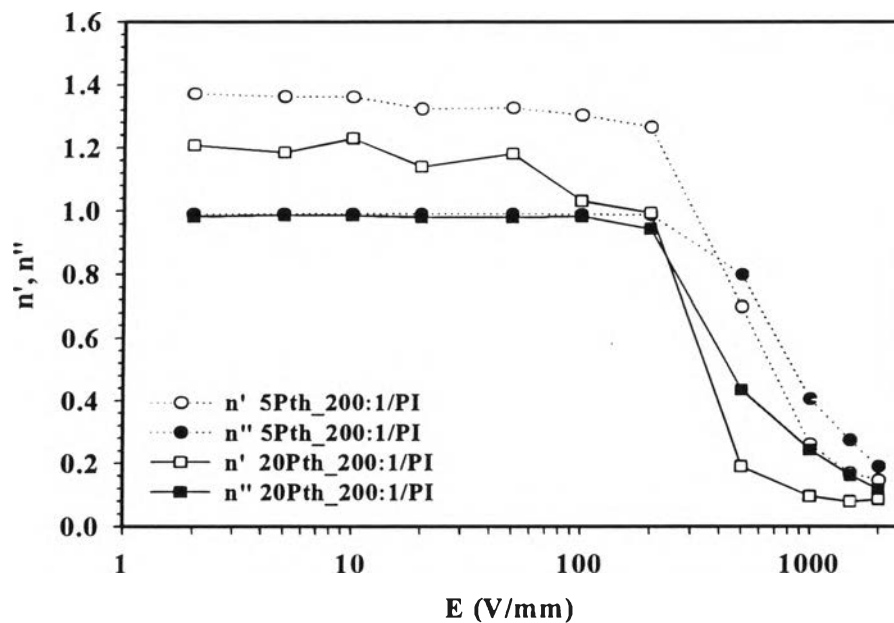


(b)

Figure 5.7 Storage modulus ($\Delta G'$) and loss modulus responses ($\Delta G''$) of HClO_4 highly doped polythiophene/polyisoprene suspensions as functions of particle concentration, 27°C , at various frequencies, and at electric field strengths of 1 and 2 kV/mm.

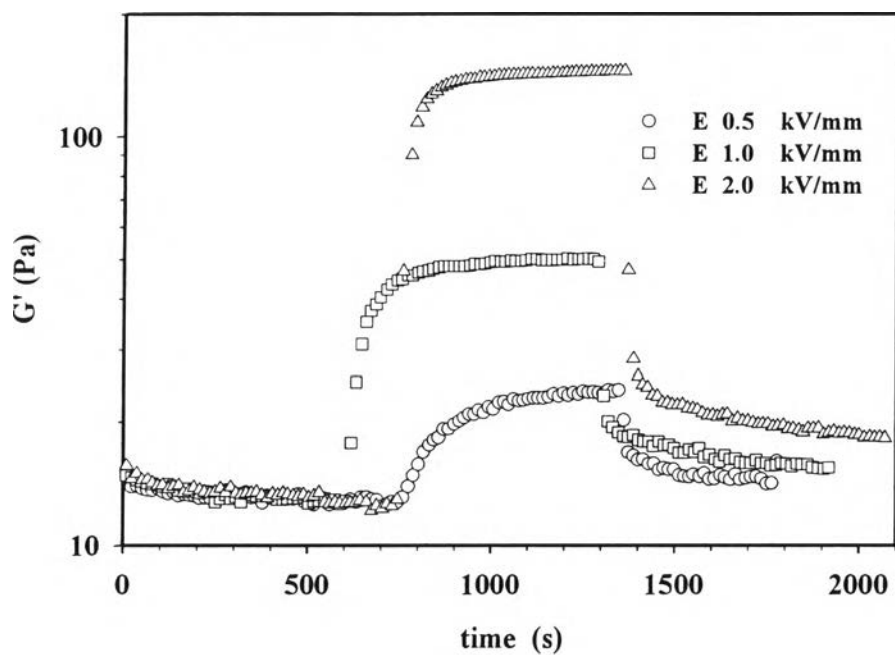


(a)

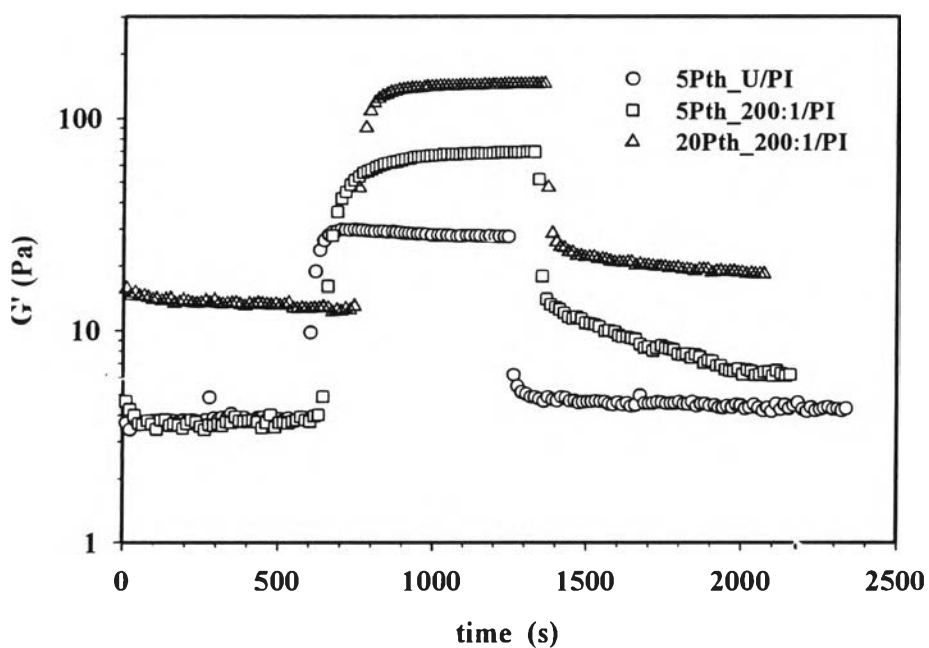


(b)

Figure 5.8 The scaling exponents n' and n'' vs. electric field strength of HClO_4 doped polythiophene/polyisoprene suspensions, and at temperature of 27°C : (a) Undoped and highly doped, 5 vol.%; (b) Highly doped at various particle concentrations.



(a)



(b)

Figure 5.9 Temporal response of storage modulus (G') of: (a) 20 vol.% HClO_4 highly doped polythiophene/polyisoprene suspensions (20Pth_200:1/PI) at various electric field strengths; (b) Polythiophene/polyisoprene suspensions at various doping ratio and particle concentration, electric field strength of 2 kV/mm, at 27°C.